JOURNAL OF Materials CHEMISTRY

Crystal structures and optical properties of cation radical salts of a tetrathiafulvalene trisannulated macrocycle

Tomoyuki Akutagawa,*[a,b,c] Yukako Abe,[c] Tatsuo Hasegawa,[a,c] Takayoshi Nakamura,*[a,c] Tamotsu Inabe,[d] Ken-ich Sugiura,[e] Yoshiteru Sakata,[e] Christian A. Christensen,[f] Jesper Lau[f] and Jan Becher[f]

[a]*Research Institute for Electronic Science, Hokkaido University, Sapporo 060-0812, Japan*
[b]*PRESTO, Japan Science and Technology Corporation (JST), Japan*
[c]*Graduate School of Environmental Earth Science, Hokkaido University, Sapporo 060-0810, Japan*
[d]*Department of Chemistry, Faculty of Science, Hokkaido University, Sapporo 060-0810, Japan*
[e]*Institute of Scientific and Industrial Research, Osaka University, Ibaraki, Osaka 567-0047, Japan*
[f]*Department of Chemistry, Odense University, Campusvej 55, DK-5230 Odense M, Denmark*

Received 5th July 1999, Accepted 31st August 1999

Cation radical salts of the bis(methylthio)tetrathiafulvalene (DMT-TTF) trisannulated macrocycles, [tris(DMT-TTF)]I_3^- (**1**) and [tris(DMT-TTF)]IBr_2^- (**2**), were prepared and the crystal structures and polarized reflectance spectra of the salts **1** and **2** were investigated. An isostructural character is observed for the two salts. The C_3 symmetry of tris(DMT-TTF) bearing three equivalent DMT-TTF units (**A**, **B**, and **C**) within a molecule is broken through the formation of cation radical salts. Two DMT-TTF units (**B** and **C**) of three equivalent units form an intramolecular dimer structure through the face-to-face π–π overlap, whereas the plane of the **A** unit is orthogonal to the dimer plane and isolated from the other units. The intramolecular dimers are further dimerized through the intermolecular **B**–**B**′ interaction, resulting in a DMT-TTF tetramer unit (**C**–**B**–**B**′–**C**′) within the crystal. The intramolecular bond lengths and polarized reflectance spectra indicate the localization of a unit charge on the **B** unit rather than **A** or **C**. The charge separated $\mathbf{A}^0$–$\mathbf{B}^+$–$\mathbf{C}^0$ electronic structure is confirmed.

Introduction

A large number of organic metals and superconductors have been reported in the forms of cation radical salts and charge-transfer (CT) complexes using tetrathiafulvalene (TTF) based electron donor molecules.[1] TTF molecules have a tendency to assemble in one-dimensional stacks through π–π overlaps along the stacking direction.[1a] The TTF systems are easily oxidized by chemical or electrochemical oxidation procedures,[1b] and the regular stack of partially oxidized TTF molecules provides partially filled one-dimensional π-band structures resulting in metallic electrical conduction properties.[1a,b] TTF derivatives can also interact in a side-by-side manner through the overlap of atomic orbitals of the peripheral sulfur atoms, which increases the dimensionality of the π-band structure along the transverse direction.[1c] The bis(ethylenedithio)tetrathiafulvalene (BEDT-TTF) molecule in particular has an ability to increase the transverse interactions and provides a large number of organic metals and superconductors with two-dimensional electronic structures.[1c,2] A large number of TTF derivatives have been prepared by chemical modifications of the BEDT-TTF molecule giving rise to novel organic metals and superconductors.[2]

TTF annulated macrocycles are interesting molecular systems for constructing new molecular electronic materials, considering the possibility for three dimensional molecular interactions in oligo-TTF systems.[3] The development of the cyanoethylene protection–deprotection protocol opens the field of synthesis of multi TTF macrocycles.[4] Complicated molecular systems such as cyclophane,[5] catenane,[6] and oligomeric[7] TTF derivatives have been synthesized. Such multi-TTF macrocycles have multiple redox active TTF units and structurally flexible macrocyclic parts within the same molecule. Since the packing arrangement of redox active TTF units should be structurally restricted by the intramolecular bridging units, unique stacking arrangements or intermolecular interactions in the crystalline face are expected when these macrocycles are used as electron donors in organic conductors. Although this unique packing should provide novel electronic structures and properties, the crystal structures and physical properties of these TTF multiannulated macrocycles, especially with the open-shell electronic structure, have not been studied extensively. In a previous paper, we have reported the crystal structure and optical properties of a TTF bisannulated macrocycle in the open-shell electronic state and found that the Z-type conformation with divalent cation state was one of the typical characteristics in the TTF bisannulated macrocycle.[8]

In the case of a TTF trisannulated macrocycle,[7a] three redox active TTF units exist within the molecule and complicated molecular conformations in the crystal are expected. Recently, a criss-cross tris-TTF cyclophane with C_1 symmetry has been reported.[9] The crystal structures of this neutral donor molecule and cation radical salt of the I_3^- counter anion showed redox active conformational change.[9] We employed here the tris(DMT-TTF) having C_3 molecular symmetry as a TTF trisannulated macrocycle (Chart 1).[7a] The linkers between three DMT-TTF units are propyldithio groups, –S–$(CH_2)_3$–S–. One interesting question is whether the TTF trisannulated macrocycle with an open-shell electronic structure has planar C_3 symmetry or non-centrosymmetry in the solid state. The molecular conformation is closely related to the charge

Table 1 Crystal data, data collection, and reduction parameters of [tris(DMT-TTF)](I_3^-)(DCE)$_{1.5}$ (**1**) and [tris(DMT-TTF)](IBr_2^-)(DCE)$_{1.5}$ (**2**)

	1	**2**
Formula	$C_{39}H_{42}S_{24}I_3Cl_3$	$C_{36}H_{42}S_{24}Cl_3Br_2I$
Formula weight	1767.27	1637.24
Crystal system	Triclinic	Triclinic
Space group	$P\bar{1}$ (no. 2)	$P\bar{1}$ (no. 2)
Crystal size/mm^3	$0.5\times0.2\times0.1$	$0.6\times0.4\times0.1$
a/Å	13.653(2)	13.656(5)
b/Å	20.303(3)	20.254(4)
c/Å	12.677(1)	12.638(4)
α/°	104.622(10)	104.75(2)
β/°	116.501(7)	116.18(3)
γ/°	81.65(1)	81.57(2)
U/Å^3	3040.8(6)	3031(1)
Z	2	2
T/K	190 K	190 K
D_{calc}/g cm^{-3}	1.930	1.794
F(000)	1740.0	1632.0
μ/cm^{-1}	25.30	28.39
$2\theta_{max}$/°	55.0	55.0
Total reflections measured	14557	14538
Unique reflections	13972	13955
No. of observations	6563	10238
No. of refined parameters	595	595
$(\Delta\rho)_{max}$/e Å^{-3}	2.02	4.55
$(\Delta\rho)_{max}$/e Å^{-3}	−1.52	−2.37
R	0.073	0.079
R_w	0.079	0.088

distribution on the TTF units and thus to the electronic and optical properties of the crystal. We report here the crystal structures and optical properties of cation radical salts based on the tris(DMT-TTF) molecule and discuss the charge population within the molecule in connection with the optical properties of the crystal.

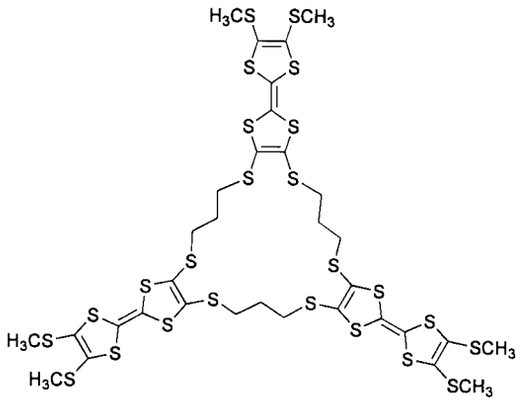

Chart 1

Experimental

Preparation of cation radical salts

The TTF trisannulated macrocycle, tris(DMT-TTF), was prepared using the cyanoethylene protection–deprotection protocol according to the literature.[7a] The single crystals of cation radical salts were grown using the standard electrocrystallization method. The electrocrystallization solvent, 1,2-dichloroethane (DCE), was distilled under argon and was passed through a neutral alumina column prior to use. A constant current (2 μA) was applied to the platinum electrodes (1 mm diameter) equipped with the H-shaped cell (18 ml) for two weeks at room temperature. The electrocrystallization using the supporting electrolytes of n-$(C_4H_9)_4N{\cdot}I_3$ or n-$(C_4H_9)_4N{\cdot}IBr_2$ provided high-quality single crystals, while the formation of crystalline solid was not observed using the electrolytes of n-$(C_4H_9)_4N{\cdot}F$, n-$(C_4H_9)_4N{\cdot}Cl$, n-$(C_4H_9)_4N{\cdot}Br$, n-$(C_4H_9)_4N{\cdot}I$, n-$(C_4H_9)_4N{\cdot}BF_4$, n-$(C_4H_9)_4N{\cdot}ClO_4$, or n-$(C_4H_9)_4N{\cdot}PF_6$ under the same conditions. The stoichiometries of the radical salts were determined by X-ray structural analysis as [tris(DMT-TTF)](I_3^-)(DCE)$_{1.5}$ (**1**) and [tris(DMT-TTF)](IBr_2^-)(DCE)$_{1.5}$ (**2**), respectively. The single crystals **1** and **2** were black plates with typical dimensions of $1.5\times0.5\times0.1$ and $0.5\times0.2\times0.05$ mm^3, respectively.

†CCDC reference number 1145/182. See http://www.rsc.org/suppdata/jm/1999/2737 for crystallographic files in .cif format.

Table 2 Selected bond lengths (Å) in the tris(DMT-TTF) **A**, **B**, and **C** units[a]

	A	**B**	**C**
1			
a: C=C	C5–C6 = 1.37(2)	C13–C14 = 1.36(2)	C24–C25 = 1.37(2)
b: C–S	S1–C5 = 1.76(1)	S9–C14 = 1.72(1)	S17–C25 = 1.75(1)
	S2–C6 = 1.75(1)	S10–C13 = 1.74(1)	S18–C24 = 1.75(1)
	S5–C6 = 1.76(1)	S13–C13 = 1.74(1)	S21–C24 = 1.74(1)
	S6–C5 = 1.76(1)	S14–C14 = 1.71(1)	S22–C25 = 1.75(1)
c: S–C	S1–C2 = 1.76(1)	S9–C18 = 1.72(1)	S17–C28 = 1.77(2)
	S2–C7 = 1.77(2)	S10–C19 = 1.76(1)	S18–C30 = 1.75(1)
	S5–C8 = 1.79(2)	S13–C12 = 1.75(1)	S21–C23 = 1.77(1)
	S6–C3 = 1.79(2)	S14–C15 = 1.74(1)	S22–C26 = 1.77(1)
d: C=C	C2–C3 = 1.30(2)	C12–C19 = 1.36(2)	C23–C30 = 1.33(2)
	C7–C8 = 1.29(2)	C15–C18 = 1.36(2)	C26–C28 = 1.34(2)
2	**A**	**B**	**C**
a: C=C	C5–C6 = 1.34(1)	C13–C14 = 1.39(1)	C24–C25 = 1.35(1)
b: C–S	S1–C5 = 1.760(9)	S9–C14 = 1.716(9)	S17–C25 = 1.746(9)
	S2–C6 = 1.768(9)	S10–C13 = 1.740(9)	S18–C24 = 1.758(9)
	S5–C6 = 1.770(9)	S13–C13 = 1.721(9)	S21–C24 = 1.761(9)
	S6–C5 = 1.757(9)	S14–C14 = 1.726(9)	S22–C25 = 1.766(9)
c: S–C	S1–C2 = 1.761(9)	S9–C18 = 1.745(8)	S17–C28 = 1.769(9)
	S2–C7 = 1.765(9)	S10–C19 = 1.747(8)	S18–C30 = 1.766(8)
	S5–C8 = 1.765(9)	S13–C12 = 1.737(8)	S21–C23 = 1.772(9)
	S6–C3 = 1.765(9)	S14–C15 = 1.736(8)	S22–C26 = 1.770(8)
d: C=C	C2–C2 = 1.36(1)	C12–C19 = 1.35(1)	C23–C30 = 1.34(1)
	C7–C8 = 1.34(1)	C15–C18 = 1.36(1)	C26–C28 = 1.35(1)

[a]atomic numbering scheme is illustrated in Fig. 1. Bonds a, b, c, and d are as shown:

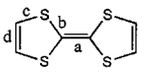

Crystal structure determinations†

Crystal data of the salts **1** and **2** were collected on a Rigaku AFC-7R diffractometer with Mo-Kα ($\lambda = 0.71073$ Å) radiation using a graphite monochromator. The unit cell parameters were determined and refined from 25 reflections. Data were collected with the 2θ–ω scan mode (scan rate = 16° min^{-1}). Lorentz polarization and absorption corrections applied with $I > 3.00\sigma(I)$ were used in refinement. The structure refinements were performed by the full matrix least-squares method. Calculations were performed using teXsan[10] crystallographic software packages with refinements based F^2. Table 1 summarizes the crystal data. Parameters were refined using anisotropic temperature factors in all crystals, and the hydrogen atoms were removed from the refinements. Table 2 summarizes the selected bond lengths.

Optical spectra

Polarized reflectance spectra were measured on single crystal samples at 296 K using a grating monochromator (5000–30 000 cm^{-1}) and a Fourier-transform infrared spectrometer (1000–5000 cm^{-1}). The reflectance spectra were observed for the incident beams polarized parallel ($E\|$) and orthogonal ($E\perp$) to the $a+b$ axis.

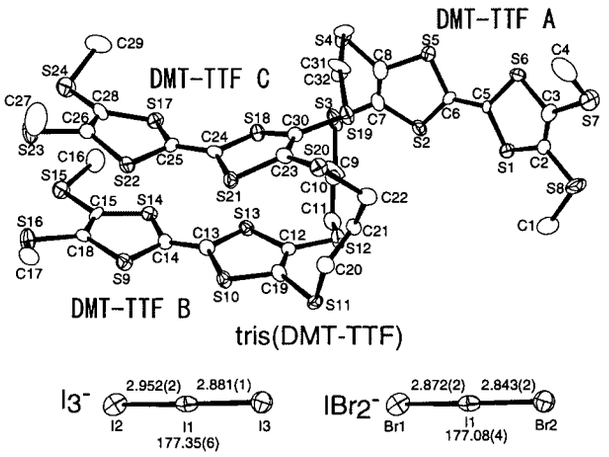

Fig. 1 Molecular structure of tris(DMT-TTF) and counter anions (I_3 and IBr_2) in the salts **1** and **2**. The tris(DMT-TTF) molecule bears three DMT-TTF units **A**, **B**, and **C**.

Calculation of transfer integral

The transfer integrals (t) were calculated within the tight-binding approximation using the extended Hückel molecular orbital calculation. The HOMO of the tris(DMT-TTF) molecule was used as a basis function.[11] The semiempirical parameters for Slater-type atomic orbitals were taken from ref. 11. The t value between each pair of molecules is assumed to be proportional to the overlap integral (s), $t = Es$, where E is a constant of -10.0 eV. The transfer integrals were calculated by assuming three independent tetrakis(methylthio)TTF molecules. Since the π-conjugation between three DMT-TTF units **A**, **B**, and **C** is disrupted by the propyl linkers, the HOMOs of the **A**, **B**, and **C** units should be independent of each other (see below).

Results and discussion

Crystal structures

The cation radical salts, [tris(DMT-TTF)](I_3^-)$(DCE)_{1.5}$ (**1**) and [tris(DMT-TTF)](IBr_2^-)$(DCE)_{1.5}$ (**2**), are isostructural with each other. The unit cell volume of the latter salt is about 10 Å^3 smaller than that of the former due to the smaller size of the counter anion IBr_2. Fig. 1 shows the crystallographically independent molecules of one tris(DMT-TTF) and one I_3^- (IBr_2^-).

The three kinds of DMT-TTF units, **A**, **B**, and **C**, are crystallographically independent within a molecule. A non-planar conformation through the folding of the central propyl linkers is observed. As a result, the C_3 molecular symmetry of tris(DMT-TTF) is broken in the cation radical state. Each DMT-TTF unit **A**, **B**, and **C** has an independent π-electronic structure due to non-conjugation at the propyl linkers. The molecular plane of the **B** unit is parallel to that of **C**, while that of the **A** unit is orthogonal to those of **B** and **C**. A pair of **B** and **C** units form an intramolecular dimer structure through face-to-face π–π overlap with the intramolecular S–S contacts shorter than the van der Waals interaction.[12] The **A** unit is completely isolated from the **B** and **C** units without intramolecular interactions. The counter anions, I_3^- and IBr_2^-, have almost linear conformation with the central I–I–I and Br–I–Br angles of 177.35(6) and 177.08(4)°, respectively. Slight asymmetries of I–I and I–Br bond lengths within the I_3 and IBr_2 anions are observed in the I–I and I–Br intramolecular distances [I1–I2 = 2.952(2) and I1–I3 = 2.881(1) Å; I1–Br1 = 2.872(2) and I1–Br2 = 2.843(1) Å].

Fig. 2 shows the stereoview of the unit cell of the salt **1** viewed along the c-axis. The intramolecular dimer pairs of **B–C** are further dimerized in the stacking order of **C–B–B′–C′** along the $a+b$ axis, where the prime symbol indicates the molecules generated by the inversion center. Each tetramer is isolated without further effective face-to-face interactions along the

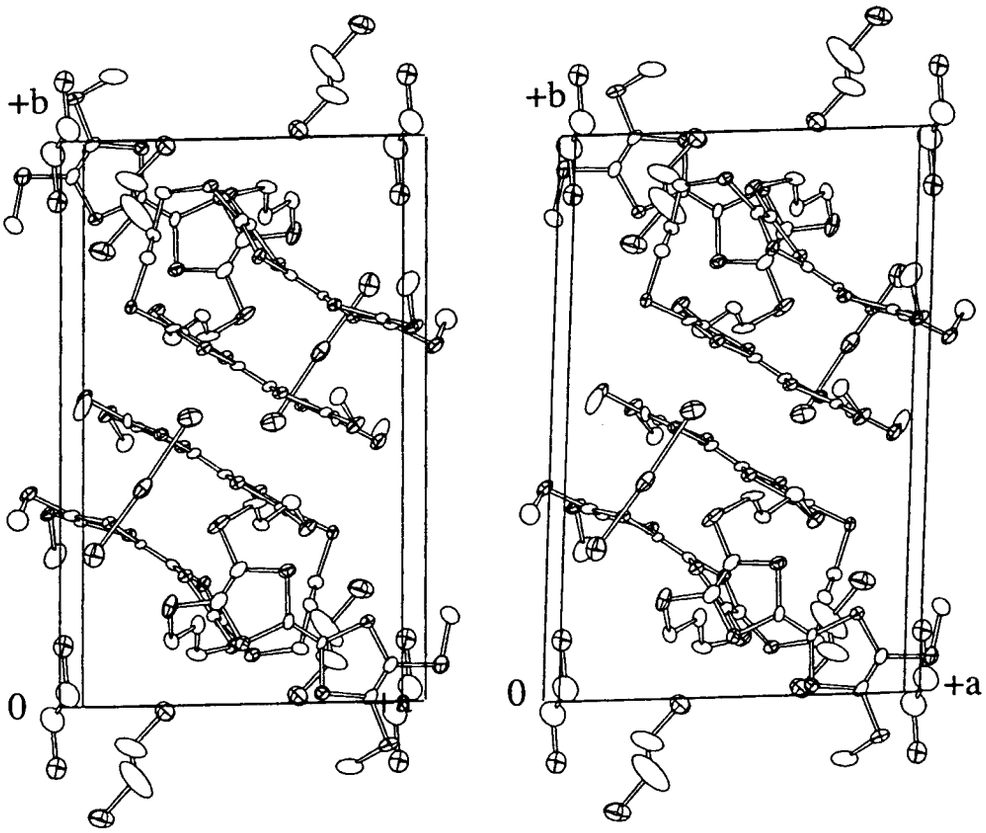

Fig. 2 Stereoview of the unit cell of the salt **1** viewed along the c-axis.

$a+b$ direction, which is consistent with the insulating electrical conducting behavior of the crystals (room temperature conductivity was below 10^{-7} S cm^{-1} for the salts **1** and **2**). The counter anions I_3^- and IBr_2^- are embedded on the **B–C** dimer of each molecule and are parallel to the stacking direction of the tetramer. The counter anions are isolated from each other. Weak interatomic I–S (*ca.* 3.89 Å) and Br–S (*ca.* 3.87 Å) contacts are observed between the counter anions and the **B** unit, which distances are *ca.* 0.2 Å longer than the van der Waals contacts.[12] Two kinds of crystallographically independent solvent molecules, 1,2-dichloroethane (DCE) **D** and **E**, were found in the crystals. The **E** molecule locates on an inversion center. Since the average isotropic thermal parameter of DCE molecules ($B_{eq} \approx 9$) is quite large, DCE molecules should be disordered within the crystal even at 190 K. One and a half DCE molecules are necessary to fill the unit cell of the tris(DMT-TTF)I_3^- and tris(DMT-TTF)IBr_2^- within the crystal. The molecular packing for each DMT-TTF unit within the crystal is restricted due to the intramolecular linkage structure compared with TTF monomer. As a result, the crystal formation largely depends on the sizes and shapes of counter anions and/or solvent molecules. The TTF multiannulated macrocycle, which takes a unique conformation in the solid state, needs appropriate counter anions and solvent molecules to fill the space in the crystal.

The π–π overlap modes of the **B–C** and **B–B′** pairs are ring over ring type. Fig. 3a shows the packing arrangement of the tetramer units viewed along the short axis of the **B** unit. Table 3 summarizes the mean interplanar distances between the **B–C** (d_1/Å) and **B–B′** (d_2/Å) pairs and transfer integrals (t_1–t_7 $\times 10^{-2}$ eV) of the salts **1** and **2**. The mean interplanar distances in the intradimer **B–C** pair ($d_1 = 3.485$ and 3.184 Å for the salts **1** and **2**, respectively) are shorter than that of the interdimer **B–B′** distances ($d_2 = 3.561$ and 3.554 Å for the salts **1** and **2**, respectively). However, the transfer integral in the **B–B′** pair ($t_2 = -36.9$ and -37.6 for the salts **1** and **2**, respectively) is larger than that of the former **B–C** pair ($t_1 = 22.3$ and 22.7 for the salts **1** and **2**, respectively). The magnitude of dimerization within a molecule is *ca.* 60% smaller than that of the intermolecular overlap, which is due to the molecular conformation and the charged state of the **B** and **C** units (see below). The intermolecular **B–B′** interaction is the most prominent interaction within the crystal.

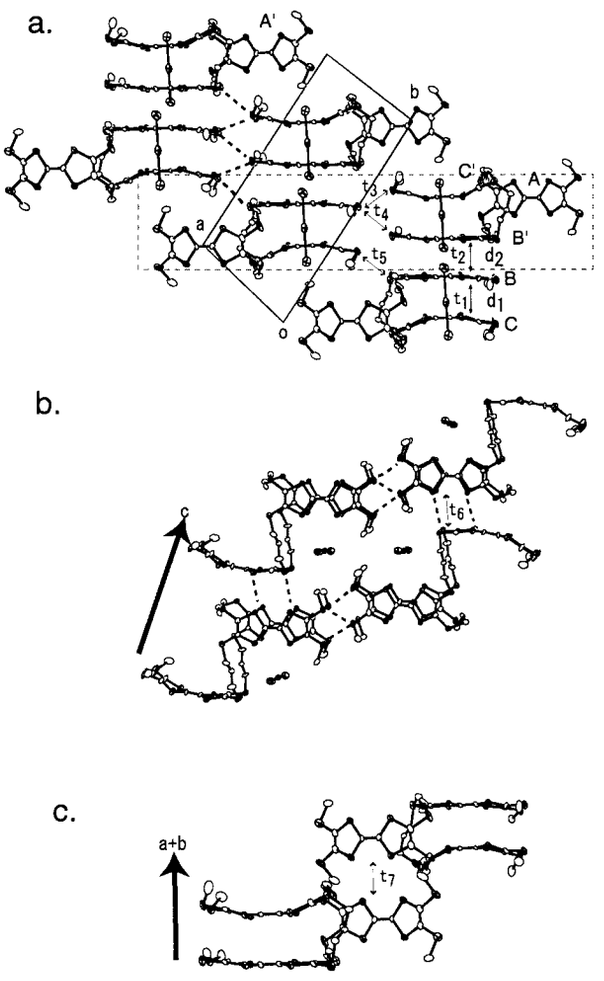

Fig. 3 Intramolecular and intermolecular π–π interactions for the salt **1**. a) Tetramer units **C–B–B′–C** viewed along the short axis of the DMT-TTF **B**. The molecules enclosed by dashed lines correspond to those depicted in Fig. 3b. b) Packing arrangement of DMT-TTF viewed normal to the molecular plane of the DMT-TTF **B**. c) Side-by-side intermolecular interaction normal to the DMT-TTF **A** unit.

Both salts have a 3 : 1 ratio of the donor and anion molecules. A unit charge should be on the [tris(DMT-TTF)]$^+$ molecule. Since three DMT-TTF units can accept the positive charges independently, several charge distribution modes are possible. The delocalization of the charge over all three DMT-TTF units is not reasonable since the conjugation is disrupted at the propyl linker. Three modes are mainly considered to distribute the unit charge on the tris(DMT-TTF) molecule; i) localization of the unit charge on the $\mathbf{A}^+$, $\mathbf{B}^+$, or $\mathbf{C}^+$ unit, ii) delocalization of the unit charge on the tetramer unit $(\mathbf{C–B–B'–C'})^{2+}$, and iii) independent charge distribution on three DMT-TTF units such as $\mathbf{A}^{+0.3}$–$\mathbf{B}^{+0.4}$–$\mathbf{C}^{+0.3}$. Among these, the charge localized state of $\mathbf{A}^0$–$\mathbf{B}^+$–$\mathbf{C}^0$ is the most reasonable electronic structure based on the structural analysis of DMT-TTF units and optical spectra.

Fig. 3b shows the packing arrangement of the tris(DMT-TTF) within the same plane enclosed in dashed lines of Fig. 3a. The conformations of DMT-TTF **A**, **B**, and **C** units within a molecule are different to each other. Both the **A** and **C** units have a similar conformation bending at the terminal –S–C=C–S– part in the TTF framework, while the **B** unit has an almost planar conformation. The non-planar conformation reported in the neutral TTF molecule[13] is close to those of the **A** and **C** units. On the other hand, the TTF^+ has a planar conformation[13] suggesting that the **B** unit is in an oxidized electronic state. Table 4 summarizes the average C=C (a), C–S (b), S–C (c), and C=C (d) bond lengths assuming D_h symmetry of TTF units together with those of neutral $(BEDT\text{-}TTF)^0$ and monovalent $(BEDT\text{-}TTF)^{+1}$. The bond lengths within the TTF molecular framework are sensitive to its charged state. It has been reported that the C=C double bonds (a and d in Table 2) become longer and the C–S single bonds (b and c in Table 2) become shorter as compared with neutral TTF^0 on oxidation.[13,14] For the salt **2**, the average C–S (b) and S–C (c) bond lengths in the **A** and **C** units are 0.02–0.03 Å longer than those

Table 3 Mean interplanar distances of DMT-TTF **B–B′** (d_1/Å) and **B–C** pairs (d_2/Å) and transfer integrals (t_1–$t_7 \times 10^{-2}$ eV) of the salts **1** and **2**[a]

	1	**2**
d_1	3.485	3.184
d_2	3.561	3.554
t_1	22.31	22.70
t_2	−36.85	−37.54
t_3	0.94	0.94
t_4	−1.20	−1.07
t_5	0.27	0.33
t_6	−0.76	−0.95
t_7	3.50	0.42

[a]Mean interplanar distances are determined from 10 atoms of the TTF unit. The transfer integrals are obtained based on the HOMO of the tris(DMT-TTF) molecule using extended Hückel molecular orbital calculations.

Table 4 Average bond lengths (Å) of each of the DMT-TTF units **A**, **B**, and **C** in the salts **1** and **2** together with neutral $(BEDT\text{-}TTF)^0$ and monovalent $(BEDT\text{-}TTF)^{+1}$ ReO_4[a]

	1			**2**				
	A	**B**	**C**	**A**	**B**	**C**	$BEDT\text{-}TTF^0$	$(BEDT\text{-}TTF)ReO_4$
a: C=C	1.37	1.36	1.37	1.34	1.39	1.35	1.31	1.38
b: C–S	1.76	1.73	1.75	1.76	1.73	1.76	1.757	1.72
c: S–C	1.78	1.74	1.77	1.77	1.74	1.77	1.754	1.73
d: C=C	1.30	1.36	1.35	1.35	1.36	1.35	1.332	1.37

[a]The bond lengths a, b, c, and d are averaged by assuming D_{2h} symmetry. The data of neutral $(BEDT\text{-}TTF)^0$ and fully ionized $(BEDT\text{-}TTF)^{+1}$ are taken from ref. 15. Bonds a, b, c, and d are as shown for Table 2.

of the **B** unit. In addition, the C=C (a and d) bond lengths in the **A** and **C** units for the salt **2** are slightly shorter than those in the **B** unit. The same tendencies in the C–S and C=C bond lengths by the oxidation of the neutral BEDT-TTF molecule have been reported in the fully ionized $(BEDT\text{-}TTF)ReO_4(THF)_{0.5}$ salt.[15] Since the intramolecular bond lengths of the **B** unit are close to that of the $(BEDT\text{-}TTF)^+$ salt rather than the neutral $(BEDT\text{-}TTF)^0$, the charged states in the **B** unit for the salt **2** should be close to the fully ionized $\mathbf{B}^+$ state. On the other hand, the bond lengths in the **A** and **C** units are close to those of the neutral state found in the $(BEDT\text{-}TTF)^0$. The C=C bond length (a) for the salt **1** is not consistent with the above estimation, however, the isostructural molecular conformation with the salt **2** and optical spectra (see the section on optical properties) are consistent with the fully ionized $\mathbf{B}^+$ state for the salt **1**. From these results we can conclude that the charge population on the tris(DMT-TTF) molecule is the charge-separated $\mathbf{A}^0$–$\mathbf{B}^+$–$\mathbf{C}^0$ electronic state rather than the $\mathbf{A}^+$–$\mathbf{B}^0$–$\mathbf{C}^0$, $\mathbf{A}^0$–$\mathbf{B}^0$–$\mathbf{C}^+$ or mixed valence $\mathbf{A}^{+\delta}$–$\mathbf{B}^{+\delta}$–$\mathbf{C}^{+\delta}$ states. The charge separated $\mathbf{A}^0$–$\mathbf{B}^+$–$\mathbf{C}^0$ molecules are further dimerized at the $\mathbf{B}^+$–$\mathbf{B}^+$ pair, forming a $\mathbf{C}^0$–$\mathbf{B}^+$–$\mathbf{B}'^+$–$\mathbf{C}'^0$ tetramer.

Each tetramer unit is connected by three kinds of weak intermolecular interactions along the *a*- (t_4 and t_5) and *b*- (t_3) axis, respectively. Since the intertetramer interactions are only observed at the terminal sulfur atoms, the magnitudes of these interactions in the salts **1** ($t_3=0.94$, $t_4=-1.20$, and $t_5=0.27$) and **2** ($t_3=0.94$, $t_4=-1.07$, and $t_5=0.33$) are significantly smaller than those of the intratetramer (t_1 and t_2). Additional intermolecular interaction (t_6) between the intramolecular **B**–**C** dimer and the isolated **A** unit is observed for the face to side overlap mode, which connected the tris(DMT-TTF) molecules along the *c*-axis (Fig. 3b). Such an orthogonal intermolecular interaction of the π-orbital has been observed in the κ-type structure in the BEDT-TTF salts. A number of molecular superconductors have been obtained from the κ-type salts.[1c,2] The magnitude of t_6 interaction found in the salts **1** ($t_6=-0.76$) and **2** ($t_6=-0.95$) is not effective in increasing the intermolecular interaction along the *c*-axis, however. The counter anions exist within the cage surrounded by four tris(DMT-TTF) molecules. Finally, the intermolecular interaction (t_7) is observed for the side-by-side contact between the **A** units along the $a+b$ axis. The magnitude of side-by-side interaction in the salt **1** ($t_7=3.50$) is larger than that in the salt **2** ($t_7=0.42$). The existence of two types of orthogonal DMT-TTF planes complicates the intermolecular interaction scheme and provides the multi-dimensional π–π interactions within the crystal. Since the charge is mainly localized on the **B** unit, three-dimensional π–π interactions could not contribute to the electrical conduction.

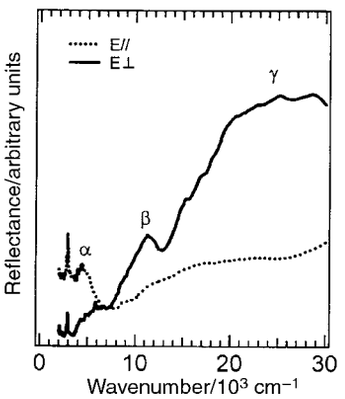

Fig. 4 Polarized reflectance spectra of the salt **1** in the energy range from 1000 to 30 000 cm^{-1}. Polarization spectra are measured with the electric vector parallel ($E\|$) and normal ($E\perp$) to the $a+b$ axis.

Optical properties

Fig. 4 shows the polarized reflectance spectra of a single crystal **1** in the energy range from 1000 to 30 000 cm^{-1}. The reflectance spectra were measured with the electric vector parallel ($E\|$) and perpendicular ($E\perp$) to the incident plane along the $a+b$ axis. Since the tetramer is elongated along the $a+b$ axis, the reflectance spectra with $E\|$ arrangement reveal the interunit transitions within the tetramer. On the other hand, the intraunit π–π* transition moment of the DMT-TTF molecule is polarized along the long axis of the DMT-TTF molecule, which should be observed in the $E\perp$ arrangement.

The reflectance spectrum with $E\|$ arrangement shows a broad band at around 4000 cm^{-1} (α-band). The α-band is only observed in the reflectance spectra of the $E\|$ arrangement, the transition moment of which is consistent with the stacking direction of the $\mathbf{C}^0$–$\mathbf{B}^+$–$\mathbf{B}^+$–$\mathbf{C}^0$ units. The low energy α-band is assigned to the CT transition between the DMT-TTF units.[16] The isolated TTF^+ dimer in the fully ionized $(TTF^+)Br^-$ salt shows the CT transition at *ca.* 12 000 cm^{-1}, which was assigned to the intermolecular CT transition between two TTF^+ molecules. On the other hand, the partial CT salt of $(TTF^{+0.79})Br^-_{0.79}$ has the intermolecular CT transition at the lower energy region of *ca.* 4000 cm^{-1}, which was assigned to the CT transition from ionized TTF^+ to neutral TTF^0.[16] Considering the charge separated $\mathbf{A}^0$–$\mathbf{B}^+$–$\mathbf{C}^0$ electronic structure and the $\mathbf{C}^0$–$\mathbf{B}^+$–$\mathbf{B}'^+$–$\mathbf{C}'^0$ tetramer arrangement, the α-band should be assigned to the CT transition from fully ionized $\mathbf{B}^+$ to neutral $\mathbf{C}^0$ unit within the tetramer.

The origin of the β-band should be either i) intermolecular transitions from the ionized $\mathbf{B}^+$ to $\mathbf{B}'^+$ unit or ii) intramolecular transition from next HOMO to LUMO of the $\mathbf{B}^+$ unit. The latter intermolecular transition has been reported for the cation radical salts based on the BEDT-TTF molecule.[17] The former transition should appear in the reflectance spectra of the $E\|$ arrangement. However, such a band was not observed clearly in the $E\|$ arrangement. On the contrary, the band at around 12 000 cm^{-1} appears in the reflectance spectra of the $E\perp$ arrangement, which is consistent with the direction of the intramolecular transition of the DMT-TTF unit. Thus, the β-band is assigned to the intramolecular transition from next HOMO to LUMO of the fully ionized $\mathbf{B}^+$ unit. Since the γ-band is only observed in the $E\perp$ polarized arrangement, this band is assigned to the locally excited transitions of each DMT-TTF unit. The electronic structure of the $\mathbf{C}^0$–$\mathbf{B}^+$–$\mathbf{B}'^+$–$\mathbf{C}'^0$

tetramer arrangement is also confirmed by the optical measurements.

Conclusion

The cation radical salts [tris(DMT-TTF)]X^-, $X^- = I_3^-$ and IBr_2^-, were prepared by the electrocrystallization method and were isostructural to each other. Single crystals were only obtained by using the linear trihalogen anions I_3^- and IBr_2^-, while the other anions such as F^-, Cl^-, Br^-, I^-, BF_4^-, and PF_6^- provided no crystalline solid. The tris(DMT-TTF) molecule has three identical DMT-TTF units. In the solid state, the C_3 molecular symmetry of tris(DMT-TTF) is broken through the formation of an intramolecular dimer structure. The dimerized **B** and **C** units are tightly connected by the face-to-face π–π interaction. The **B**–**C** dimer pairs also form an intermolecular dimer structure (tetramer) in the stacking order **C**–**B**–**B**′–**C**′. The residual **A** unit is isolated from the **B** and **C** units within the tris(DMT-TTF) molecule and the molecular plane of the **A** unit is orthogonal to those of the **B**–**C** pair. The unit charge of the tris(DMT-TTF) is mainly localized on the **B** unit, which forms an intermolecular $\mathbf{B}^+$–$\mathbf{B}'^+$ dimer pair. The DMT-TTF units are conformationally restricted through the connection to the macrocyclic part and take a unique molecular packing in the crystal. The TTF multiannulated macrocycles gives specific conformations and molecular assemblies in the solid state. These materials will open a new possibility of applications such as higher-dimensional electronic conductors or ion–electron hybridized molecular conductors by including ions in a macrocyclic cavity. For that purpose, the design of electrically and optically active TTF multiannulated molecules from the viewpoint of supramolecular chemistry is most important.

Acknowledgements

This work was partly supported by a Grant-in-Aid for Science Research from the Ministry of Education, Science, Sports, and Culture of Japan and by the Proposal-Based New Industry Creative Type Technology R&D Promotion Program from the New Energy and Industrial Technology Development Organization (NEDO) in Japan.

References

1 (*a*) F. Wudl, *Acc. Chem. Res.*, 1984, **17**, 227; (*b*) D. O. Cowan, *New Aspects of Organic Chemistry*, ed. Z. Yoshida, T. Shiba and Y. Oshiro, Proc. 4th Int. Kyoto Conf., Kodansha Ltd, Tokyo, 1989; (*c*) G. Saito, *Metal-Insulator Transition Revisited*, ed. P. P. Edwards and C. N. R. Rao, Taylor and Francis, 1995.
2 (*a*) J. M. Williams, J. R. Ferraro, R. J. Thorn, K. D. Carlson, U. Geiser, H. H. Wang, A. M. Kini and M.-H. Whangbo, *Organic Superconductors*, Prentice-Hall, Englewood Cliffs, New Jersey, 1992; (*b*) T. Ishiguro, K. Yamaji and G. Saito, *Organic Superconductors*, ed. M. Cardona, P. Fulde, K. von Klitzing, H.-J. Queisser, Springer, 1997; (*c*) *Organic Conductors*, ed. J.-P. Farges, Marcel Dekker, New York, 1994.
3 (*a*) K. B. Simonsen and J. Becher, *Synlett*, 1997, 1211; (*b*) M. B. Nielsen and J. Becher, *Liebigs Ann./Recl.*, 1997, 2177; (*c*) T. Jørgensen, T. K. Hansen and J. Becher, *Chem. Soc. Rev.*, 1994, 41; (*d*) M. R. Bryce, *Adv. Mater.*, 1999, **11**, 11.
4 (*a*) J. Becher, J. Lau, P. Leriche, P. Mork and N. Svenstrup, *J. Chem. Soc., Chem. Commun.*, 1994, 2715; (*b*) K. B. Simonsen, N. Svenstrup, J. Lau, O. Simonsen, P. Monk, G. J. Kristensen and J. Becher, *Synthesis*, 1996, 407.
5 (*a*) T. Otsubo, Y. Aso and K. Takimiya, *Adv. Mater.*, 1996, **8**, 203; (*b*) K. Takimiya, Y. Aso, F. Ogura and T. Ostubo, *Chem. Lett.*, 1995, 735; (*c*) Z. T. Li and J. Becher, *Chem. Commun.*, 1996, 639; (*d*) Z. T. Li, P. C. Stein, J. Becher, D. Jensen, P. Mork and N. Svenstrup, *Chem. Eur. J.*, 1996, **2**, 624; (*e*) K. B. Simonsen, N. Thorup and J. Becher, *Synthesis*, 1997, 1399; (*f*) S. Yumoki, K. Takimiya, Y. Aso and T. Otsubo, *Tetrahedron Lett.*, 1997, **38**, 3071; (*g*) A. S. Batsanov, D. E. John, M. R. Bryce and J. A. Howard, *Adv. Mater.*, 1998, **10**, 1360.
6 M. B. Nielsen, Z. T. Li and J. Becher, *J. Mater. Chem.*, 1997, **7**, 1175.
7 (*a*) J. Lau and J. Becher, *Synthesis*, 1997, 1015; (*b*) G. J. Marshallsay, T. K. Hansen, A. J. Moore, M. R. Bryce and J. Becher, *Synthesis*, 1994, 926.
8 (*a*) T. Akutagawa, Y. Abe, Y. Nezu, T. Nakamura, M. Kataoka, A. Yamanaka, K. Inoue, T. Inabe, C. A. Christensen and J. Becher, *Inorg. Chem.*, 1998, **37**, 2330; (*b*) Y. Abe, T. Akutagawa, T. Hasegawa, T. Nakamura, K. Sugiura, Y. Sakata, T. Inabe, C. A. Christensen and J. Becher, *Synth. Met.*, in the press.
9 K. Takimiya, N. Thorup and J. Becher, *Chem. Eur. J.,* in the press.
10 teXsan: Single crystal structure analysis software package. Version 1.9, 1993. Molecular Structure Corporation.
11 (*a*) T. Mori, A. Kobayashi, Y. Sasaki, H. Kobayashi, G. Saito and H. Inokuchi, *Bull. Chem. Soc. Jpn.*, 1984, **57**, 627; (*b*) R. H. Summerville and R. J. Hoffmann, *J. Am. Chem. Soc.*, 1976, **98**, 7240; (*c*) A. J. Berlinsky, J. F. Carolan and L. Weiler, *Solid State Commun.*, 1974, **15**, 795.
12 A. Bondi, *J. Phys. Chem.*, 1964, **68**, 441.
13 W. F. Coopens, N. C. Kenny, J. W. Edmonds, A. Nagel, F. Wudl and P. Coppens, *J. Chem. Soc., Chem. Commun.*, 1971, 889.
14 T. J. Kistenmacher, T. E. Phillips and D. O. Cowan, *Acta Crystallogr., Sect. B*, 1974, **30**, 763.
15 H. Kobayashi, R. Kato, T. Mori, A. Kobayashi, Y. Sasaki, G. Sito, T. Enoki and H. Inokuchi, *Mol. Cryst. Liq. Cryst.*, 1984, **107**, 33.
16 J. B. Torrance, B. A. Scott, B. Welber, F. B. Kaufman and P. E. Seiden, *Phys. Rev. B.*, 1979, **19**, 730.
17 (*a*) T. Sugano, H. Hayashi, M. Kinoshita and K. Nishikida, *Phys. Rev. B.*, 1989, **39**, 11387; (*b*) T. Hasegawa, S. Kagoshima, T. Mochida, S. Sugiura and Y. Iwasa, *Solid State Commun.*, 1997, **103**, 489.

Paper 9/05362J